DOI 10.1007/s10946-023-10170-6
Journal of Russian Laser Research, Volume 44, Number 6, November, 2023

INTERACTION OF TERAHERTZ RADIATION PULSE WITH A PLASMA LAYER IN A MAGNETIC FIELD

Vyacheslav E. Grishkov,[1] Polina D. Trofimova,[2] and Sergey A. Uryupin[1,2*]

[1] *Lebedev Physical Institute, Russian Academy of Sciences*
Leninskii Prospect 53, Moscow 119991, Russia

[2] *National Research Nuclear University MEPhI (Moscow Engineering Physics Institute)*
Kashirskoe Chaussée 31, Moscow 115409, Russia

*Corresponding author e-mail: uryupin@sci.lebedev.ru

Abstract

We consider the interaction of Gaussian pulse of electromagnetic radiation with a plasma layer located in a constant magnetic field directed along the layer boundaries. We show that, when exposed to a long pulse, the transmitted pulse amplitude decreases due to a partial reflection from the layer boundaries and the influence of electron collisions. When exposed to a short pulse, in the case where the frequencies of the waves excited in the layer are far from the transparency region boundaries, the transmitted pulse broadens due to the group-velocity dispersion. If the frequencies of the excited waves are close to the transparency boundaries, the envelope oscillations appear in the transmitted pulse tail.

Keywords: terahertz pulse, magnetic field, plasma layer.

1. Introduction

The transmission of electromagnetic radiation pulses through plasma layers has been studied for a relatively long time; see, for example, [1–6]. Such studies are of interest for problems of communication with aircrafts in the upper atmosphere and for plasma diagnostics. When the aircraft moves at supersonic speed, a plasma layer is formed around the latter, making it difficult to transmit signals with frequencies lower than the plasma frequency of electrons. One way to solve this communication problem is to cover the antenna with a dielectric layer, in which the signal is resonantly amplified due to interference [5, 6]. The other proposed method is the application of an alternating magnetic field, displacing electrons and plasma ions from the antenna zone [3]. In turn, a constant magnetic field changes the plasma transparency intervals and increases the number of wave modes, the excitation of which determines the pulse propagation features in plasma. As a result, the pulse propagation features in the plasma and transmitted pulse shape change, which can be used to dynamically control the phase and shape of the pulse. Pulse shape control capabilities are important for a number of applications. Specially shaped pulses are used to control chemical reactions in the coherent control method [7] and other femtochemistry methods [8], which use devices based on diffraction gratings [9], liquid crystals [10], photonic crystals [11], and metamaterials [12, 13].

Bearing in mind the strong influence of magnetic field on the dispersion properties of plasma, in this communication, we study the interaction of a terahertz radiation pulse with a plasma layer located in a constant magnetic field. We give the expressions determining the frequency dependence of the

Manuscript submitted by the authors in English on September 28, 2023.

electromagnetic-field transmission coefficient through the plasma layer. We establish that, in the case of a sufficiently long pulse, its transmission through the plasma layer is accompanied by an amplitude decrease due to the influence of electron collisions and reflections from plasma boundaries. We show that, as the pulse duration decreases, in the case where the frequencies of the waves excited by the pulse in the plasma are sufficiently distant from the cutoff frequencies $\omega_\pm$ and ω_h, the transmitted pulse broadens due to the group velocity dispersion. When the frequencies of the excited waves are close to the frequencies $\omega_\pm$ and ω_h, oscillations appear behind the pulse caused by the nonlinear dependence of the group velocity on frequency near the cutoff frequencies $\omega_\pm$ and ω_h. For the case of a sufficiently large plasma-layer thickness, we show that changing the value of the external magnetic field strength and plasma parameters allows modulation of the transmitted signal, if the characteristic frequencies contained in the pulse are not too high compared to the plasma and cyclotron frequencies.

2. Transmitted Pulse Field

Let us consider the penetration of an electromagnetic radiation pulse through a homogeneous layer of fully ionized plasma, occupying the region $0 < x < l$ and located in an external constant magnetic field directed along the layer boundaries $\mathbf{B}_0 = (0, 0, B_0)$; see Fig. 1.

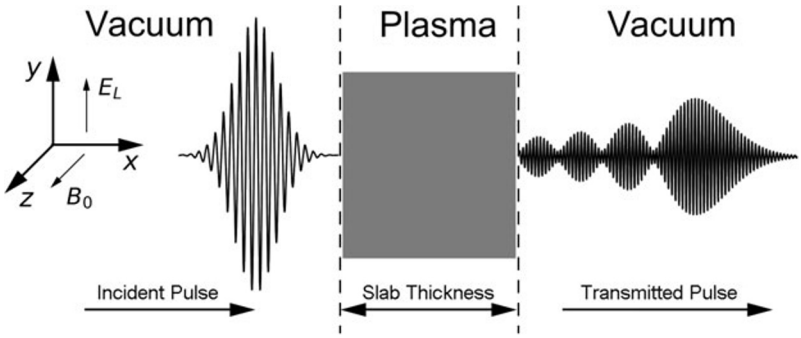

Fig. 1. Scheme of the pulse interaction with a plasma layer.

The electric field of the pulse normally incident on the plasma layer is directed transverse to the external magnetic field,

$$\mathbf{E}^{\text{inc}}(x,t) = \frac{1}{2}\mathbf{E}_L \exp\left[-\frac{(t-x/c)^2}{2t_p^2}\right] \exp\left[-i\omega_0(t-x/c)\right] + c.c., \tag{1}$$

where c is the speed of light, $\mathbf{E}_L = (0, E_L, 0)$, ω_0 is the carrier frequency, and the time t_p determines the pulse full width at half maximum according to the relationship $\tau_p = 2t_p\sqrt{\ln 2}$, with $\omega_0 t_p \gg 1$. The incident pulse field sets electrons and ions in motion. We neglect the slow movement of ions. When describing the electrons motion, we use the equation for an average electron velocity $\mathbf{u}(x,t)$,

$$\frac{\partial \mathbf{u}(x,t)}{\partial t} + \nu \mathbf{u}(x,t) = \frac{e}{m}\Big(\mathbf{E}(x,t) + \frac{1}{c}[\mathbf{u}(x,t), \mathbf{B}_0]\Big), \tag{2}$$

where e and m are the electron charge and mass, respectively, $\nu = (4/3)\sqrt{2\pi}Ze^4 n\Lambda/m^{1/2}(\kappa T)^{3/2}$ is the effective frequency of electron–ion collisions, Z is the ionization multiplicity of atom, Λ is the Coulomb logarithm, n is the electron density, κ is the Boltzmann constant, and T is the electron temperature.

The electron current density is determined by the average velocity in accordance with the relationship $\mathbf{j}(x,t) = en\mathbf{u}(x,t)$. When solving Eq. (2), we use the Fourier transform with respect to time. As a result, for the Fourier image of the current density, we have

$$j_\alpha(x,\omega) = \sigma_{\alpha\beta}(\omega) E_\beta(x,\omega), \tag{3}$$

where $\sigma_{\alpha\beta}(\omega)$ is the electrical conductivity tensor

$$\sigma_{\alpha\beta}(\omega) = \frac{\omega_p^2}{4\pi}\frac{i(\omega+i\nu)}{(\omega+i\nu)^2-\Omega^2}\Big(\delta_{\alpha\beta}+\frac{i\Omega\varepsilon_{\alpha\beta k}b_k}{\omega+i\nu}\Big), \tag{4}$$

$\omega_p = \sqrt{4\pi ne^2/m}$ is the plasma frequency of electrons, $\Omega = eB/mc$ is the cyclotron frequency, $\delta_{\alpha\beta}$ is the Kronecker symbol, $\varepsilon_{\alpha\beta k}$ is the Levi–Civita symbol, and $\mathbf{b} = (0,0,1)$ is the unit vector along the constant magnetic field.

To find the electric and magnetic fields in plasma, we use the Maxwell equations for the Fourier images of the electric $\mathbf{E}(x,\omega)$ and magnetic $\mathbf{B}(x,\omega)$ fields,

$$\nabla\times\mathbf{E}(x,\omega) = \frac{i\omega}{c}\mathbf{B}(x,\omega), \tag{5}$$

$$\nabla\times\mathbf{B}(x,\omega) = -\frac{i\omega}{c}\mathbf{E}(x,\omega)+\frac{4\pi}{c}\mathbf{j}(x,\omega). \tag{6}$$

Excluding $\mathbf{E}(x,\omega) = (0,E(x,\omega),0)$ from Eqs. (5) and (6) and using expressions for the Fourier images of the current density (3) and conductivity tensor (4) for $\mathbf{B}(x,\omega) = (0,0,B(x,\omega))$, we arrive at the equation

$$\Delta B(x,\omega)+\varkappa^2(\omega)B(x,\omega) = 0. \tag{7}$$

The characteristic wave number $\varkappa(\omega)$ [14, 15] determines the features of the pulse propagation along the OX axis in the plasma; it reads

$$\varkappa^2(\omega) = \frac{\omega^2}{c^2}\left[1-\frac{\omega_p^2-\omega(\omega+i\nu)}{\omega_p^2(\omega+i\nu)+\omega(\Omega^2-(\omega+i\nu)^2)}\cdot\frac{\omega_p^2}{\omega}\right]. \tag{8}$$

Since $B(x,-\omega) = B^*(x,\omega)$, when solving Eq. (7), it is sufficient to consider only the solution with $\omega > 0$. We look for the solution of Eq. (7) in the form of a sum of terms corresponding to the waves propagating towards each other, namely,

$$B(x,\omega) = C_1\exp\left[i\varkappa(\omega)x\right]+C_2\exp\left[-i\varkappa(\omega)x\right], \tag{9}$$

where C_1 and C_2 are unknown constants. Taking into account that $\operatorname{Im}\varkappa^2(\omega) > 0$ for $\varkappa(\omega)$, we obtain

$$\varkappa(\omega) = \frac{1}{\sqrt{2}}\Big(\sqrt{|\varkappa^2(\omega)|+\operatorname{Re}\varkappa^2(\omega)}+i\operatorname{sign}(\omega)\sqrt{|\varkappa^2(\omega)|-\operatorname{Re}\varkappa^2(\omega)}\Big). \tag{10}$$

In view of Eqs. (5) and (9), we find the Fourier image of the electric field $E(x,\omega)$ tangential component in plasma; it reads

$$E(x,\omega) = \frac{\omega}{c\varkappa(\omega)}\Big(C_1\exp\left[i\varkappa(\omega)x\right]-C_2\exp\left[-i\varkappa(\omega)x\right]\Big). \tag{11}$$

The equations for electric and magnetic fields in vacuum in regions $x < 0$ and $x > l$ are obtained from the system of equations (5) and (6), if we put $\omega_p = 0$ in (4). Moreover, in (7) $\varkappa^2(\omega) = \omega^2/c^2$. We look for the solution in the region $x < 0$ in the form $\exp\left[-i\omega x/c\right]$, which corresponds to the wave reflected from the plasma layer. In the region $x > l$, we look for a solution in the form $\exp\left[i\omega x/c\right]$, which corresponds to the transmitted wave. Confining ourselves to considering transmitted wave only and using the continuity

conditions of the tangential components of the electric and magnetic fields at the boundaries of the plasma layer $x = 0$ and $x = l$, for the field at the boundary $x = l$ we obtain

$$E(l,\omega) = B(l,\omega) = T(l,\omega)E^{\text{inc}}(0,\omega), \tag{12}$$

where $T(l,\omega)$ is the transmission coefficient of the wave with frequency ω,

$$T(l,\omega) = \frac{4\omega c\varkappa(\omega)}{\exp\left[-i\varkappa(\omega)l\right]\cdot(c\varkappa(\omega)+\omega)^2 - \exp\left[i\varkappa(\omega)l\right]\cdot(c\varkappa(\omega)-\omega)^2}, \tag{13}$$

and $E^{\text{inc}}(0,\omega)$ is the Fourier image of an incident pulse at the point $x = 0$

$$E^{\text{inc}}(0,\omega) = \frac{\sqrt{2\pi}E_L t_p}{2}\left(\exp\left[-\frac{(\omega-\omega_0)^2 t_p^2}{2}\right] + \exp\left[-\frac{(\omega+\omega_0)^2 t_p^2}{2}\right]\right). \tag{14}$$

The Fourier image of the transmitted wave field is determined by the transmission coefficient $T(l,\omega)$, which depends on the effective wave number $\varkappa(\omega)$. The value $\varkappa(\omega)$ determines the propagation features of the radiation in plasma. Frequency intervals for which $\mathrm{Re}\varkappa^2(\omega) > 0$ are the intervals of plasma transparency; for such frequencies, the propagation of an extraordinary wave is possible. In Fig. 2, we show the graph of the function $\mathrm{Re}\,\varkappa^2(\omega)c^2/\omega^2$ for $\nu = 5\cdot 10^{-2}\omega_p$ (the solid curve) and $\nu = 0$ (the dashed curve). The dash-dotted curve demonstrates the dependence of the real part of the group velocity $\mathrm{Re}\,v_g(\omega) = \left[\dfrac{d\,\mathrm{Re}\,\varkappa(\omega)}{d\omega}\right]^{-1}$ on frequency. The curves are plotted for $\Omega = 2\omega_p$.

In the case of $\nu = 0$, the real part of $\varkappa^2(\omega)$ changes sign when passing through the points $\omega_\pm = \sqrt{\omega_p^2 + \Omega^2/4} \pm \Omega/2$ and $\omega_h = \sqrt{\omega_p^2 + \Omega^2}$. Moreover, at the point ω_h, the function $\mathrm{Re}\,\varkappa^2(\omega)$ has a discontinuity. In the presence of collisions, the intervals of plasma opacity become narrower. In particular, the region of opacity, in the interval (ω_-, ω_h) at $\nu = 0$, can disappear at a sufficiently high frequency of collisions.

The coefficient $T(l,\omega)$ contains factors of the form $\exp\left[\pm i\varkappa(\omega)l\right]$ caused by multiple waves reflection from the boundaries $x = 0$ and $x = l$. The presence of these exponential factors in the function $T(l,\omega)$ leads to the appearance of oscillations in the Fourier image of the transmitted wave field $E(l,\omega)$. These

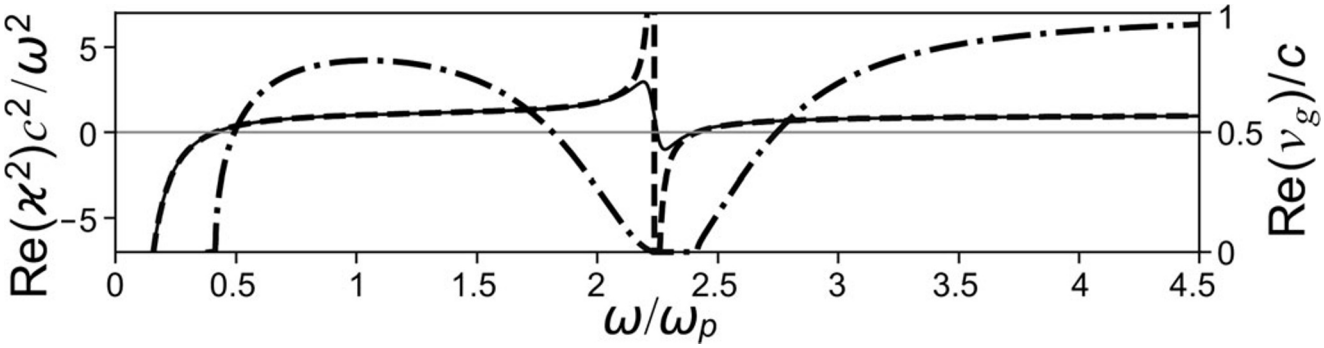

Fig. 2. Dependence of the function $\mathrm{Re}\,\varkappa^2(\omega)c^2/\omega^2$ on the frequency for $\Omega = 2\omega_p$. Here, the solid curve corresponds to $\nu = 5\cdot 10^{-2}\omega_p$, the dashed curve corresponds to $\nu = 0$, and the dash-dotted curve represents the frequency dependence of the real part of the group velocity $\mathrm{Re}\,v_g(\omega)/c$.

oscillations correspond to the time delay of the wave passing through the plasma layer relative to the wave propagating to the distance l in the vacuum. The features of the oscillations is determined by the coefficient $\varkappa(\omega)$ peculiarities: the oscillations are concentrated near the frequencies $\omega_\pm$ and ω_h, since waves excited near these frequencies have a low group velocity and their delay is the greatest.

2.1. Unmagnetized Plasma

In the absence of magnetic field, plasma is transparent to the waves with frequencies $\omega > \omega_p$ and not transparent to the waves with $\omega < \omega_p$. In numerical calculations, we consider a weakly collisional plasma with an electron density of $n = 10^{17}$ cm^{-3}, a temperature of $T = 50$ eV, and an ionization multiplicity of $Z = 1$. In this case, for the remaining plasma parameters we have

$$\omega_p = 1.8 \cdot 10^{13} \text{ s}^{-1}, \qquad \nu = 7.1 \cdot 10^9 \text{ s}^{-1}, \qquad \Lambda = \ln[(\kappa T)^{3/2}/Ze^2 m^{1/2}\omega_p] = 8.7.$$

In numerical calculations, we confine ourselves to the case of a sufficiently large plasma layer thickness l since, in the case of an optically thin layer $l \le 10c/\omega_p$, there are no noticeable changes in the pulse shape. We take the plasma layer thickness l to be equal to 0.2 cm $= 120c/\omega_p$ and assume that the plasma layer is affected by radiation with the frequency $\omega_0 = 2.0 \cdot 10^{13}$ s^{-1}.

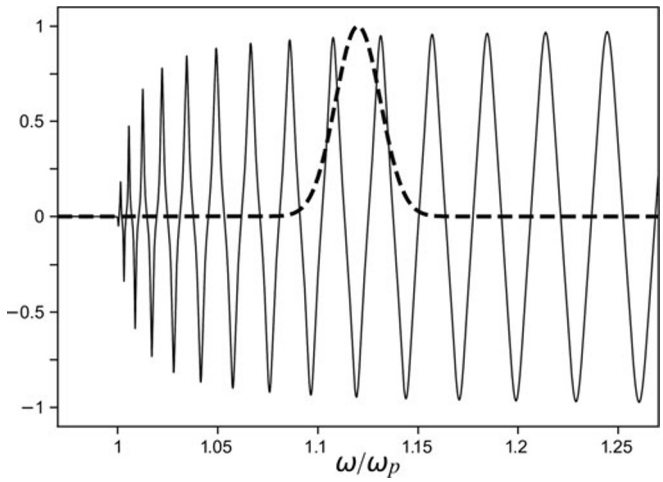

Fig. 3. The real part of transmission coefficient $T(l,\omega)$ (the solid curve) and the Fourier image of the electric component of the incident wave field $E^{\text{inc}}(0,\omega)/\sqrt{\pi/2}E_L t_p$ (the dashed curve) on the frequency. The curves are plotted for parameter values $\omega_0 = 1.12\omega_p$ and $\omega_p t_p = 89$.

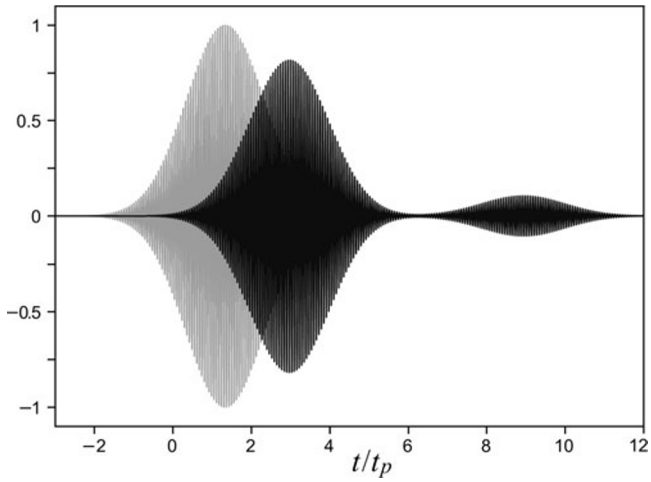

Fig. 4. Time dependences of the transmitted wave field $E(l,t)/E_L$ (the black curve) and the incident wave field $E_{\text{inc}}(l,t)/E_L$ passed the distance l in the vacuum (the gray curve). The values of plasma and pulse parameters are the same as in Fig. 3.

In Fig. 3, we show the dependences of Fourier images of the real part of transmission coefficient $T(l,\omega)$ and the incident wave field $E^{\text{inc}}(0,\omega)/\sqrt{\pi/2}E_L t_p$ on the frequency. Using the expressions for the transmitted wave electric field (12), the transmission coefficient (13) and the explicit form of the incident field Fourier image (14) after the inverse Fourier transform, we find $E(l,t)$. In Fig. 4, the gray line represents the time dependence of the electrical component of the incident pulse $E^{\text{inc}}(l,t)/E_L$ is shown by the black curve, while the black curve represents the transmitted wave field $E(l,t)/E_L$. In Figs. 3 and 4, time t_p is chosen to be equal to $5 \cdot 10^{-12}$ s $= 89/\omega_p$.

In Fig. 3, one can see that a relatively long incident pulse, having a width in the frequency range comparable to the frequency interval over which the transmission coefficient oscillation period $T(l,\omega)$ changes, excites electromagnetic waves with a similar group velocity. As a result, the shape of the pulse passing through the plasma layer changes slightly. In addition to the main pulse, there is a secondary pulse of smaller amplitude in the transmitted signal, caused by reflections from the boundaries of the plasma layer. The time delay of the secondary pulse can be estimated as $2l/v_g(\omega_0) \approx 3 \cdot 10^{-11}$ s, where $v_g(\omega_0) \simeq c\sqrt{1-\omega_p^2/\omega_0^2} \approx 0.45c$. The amplitude decrease of the secondary pulse resulting due to a double reflection from the plasma layer boundaries can be estimated as $|(\sqrt{\varepsilon}-1)/(\sqrt{\varepsilon}+1)|^2 = 0.14$, where $\varepsilon = 1-\omega_p^2/\omega_0(\omega_0+i\nu)$ is the plasma dielectric constant at the frequency ω_0.

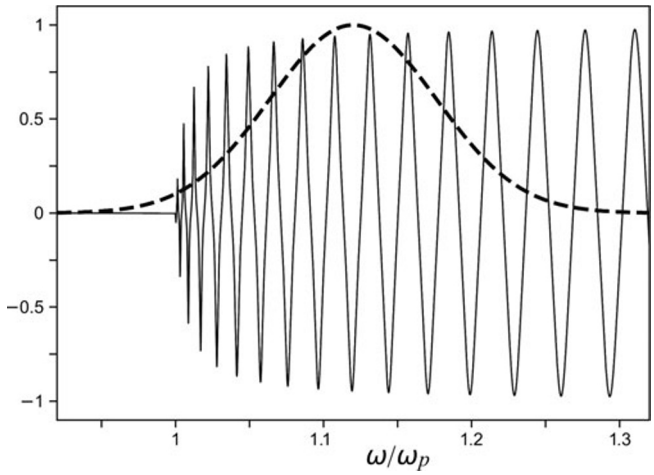

Fig. 5. The real part of transmission coefficient $T(l,\omega)$ (the solid curve) and the Fourier image of the electric component of the incident wave field $E^{\text{inc}}(0,\omega)/\sqrt{\pi/2}E_L t_p$ (the dashed curve) on the frequency. The curves are plotted for parameter values $\omega_0 = 1.12\omega_p$ and $\omega_p t_p = 18$.

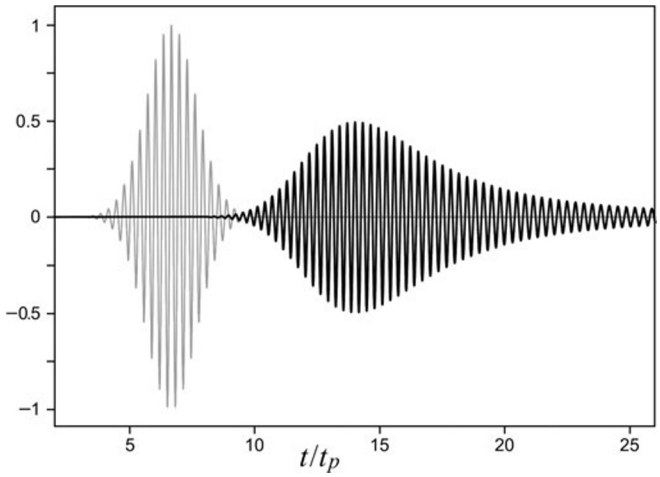

Fig. 6. Time dependences of the transmitted wave field $E(l,t)/E_L$ (the black curve) and the incident wave field $E_{\text{inc}}(l,t)/E_L$ passed the distance l in the vacuum (the gray curve). The values of plasma and pulse parameters are the same as in Fig. 5.

The dependences presented in Figs. 5 and 6 correspond to the same functions as in Figs. 3 and 4, respectively, and were built for the same plasma parameters. The pulse carrier frequency is the same as in Figs. 3 and 4, but the time t_p is 5 times smaller and equal to 10^{-12} s. Decreasing the incident pulse duration leads to a broadening of the frequency range contained in the pulse. The frequency interval broadening is accompanied by the excitation of waves with a large group velocity range and, as a consequence, transmitted pulse broadening in time.

The broadening of the pulse of the form $\exp[i\varkappa(\omega)l - (\omega-\omega_0)^2/2t_p^2]$ can be estimated by expanding the wave number $\varkappa(\omega)$ in the exponent into a Taylor series in the vicinity of the carrier frequency ω_0. Keeping only the terms quadratic in $\omega-\omega_0$ and performing the inverse Fourier transform, for a relative increase in duration we obtain $\sqrt{1+(\varkappa''(\omega_0)l)^2/t_p^4} = 3.1$.

2.2. Magnetized Plasma

In the presence of an external magnetic field, a significant change in the pulse shape can be observed compared to the case of unmagnetized plasma. Plasma placed in a constant magnetic field has two

frequency intervals of transparency (ω_-, ω_h) and (ω_+, ∞). Changing these intervals, carried out by changing the external magnetic field B_0, makes it possible to cut off the frequencies of waves passing through the plasma. In strong magnetic fields, for which the cyclotron frequency is $\Omega \gg \omega_p$, the pulse group velocity in plasma is close to the speed of light and the plasma becomes transparent. When the waves with frequencies lying in the linear dependence region of group velocity on frequency are excited, pulse broadening is observed due to group velocity dispersion. This is also true for pulses that excite waves with frequencies belonging to the interval (ω_-, ω_h), for which the group velocity varies linearly. Contra, if the incident pulse carrier frequency ω_0 belongs to the frequency interval (ω_-, ω_h), and the parameter t_p satisfies the condition $\omega_h - \omega_- \approx 4/t_p$, then the incident pulse excites waves for which the group velocity dependence on frequency is nonlinear.

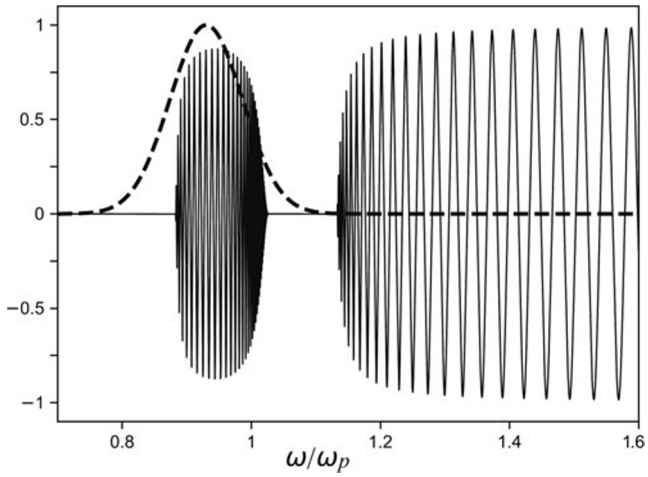

Fig. 7. The real part of transmission coefficient $T(l, \omega)$ (the solid curve) and the Fourier image of the electric component of the incident wave field $E^{\text{inc}}(0, \omega)/\sqrt{\pi/2}E_L t_p$ (the dashed curve) on the frequency. The curves are plotted for parameter values $\Omega = 0.25\omega_p$, $\omega_0 = 0.93\omega_p$, and $t_p\omega_p = 18$.

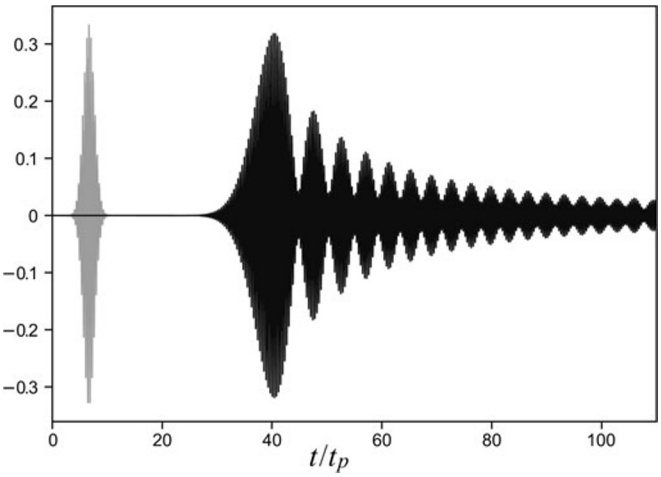

Fig. 8. Time dependences of the transmitted wave field $E(l, t)/E_L$ (the black curve) and the incident wave field $E_{\text{inc}}(l, t)/E_L$ passed the distance l in the vacuum (the gray curve). The curves are plotted for parameter values $\Omega = 0.25\omega_p$, $\omega_0 = 0.93\omega_p$, and $t_p\omega_p = 18$.

In Fig. 7, we show the same dependences as in Fig. 3, for the same plasma parameters. Graphs in Fig. 7 are plotted for the cyclotron frequency $\Omega = 0.25\omega_p$ corresponding to $B_0 = 2.5 \cdot 10^5$ G, carrier frequency $\omega_0 = 0.93\omega_p$ and time $t_p = 10^{-12}$ s, for which $t_p\omega_p = 18$. In Fig. 8, we present the same curves as Fig. 4, but for $\Omega = 0.25\omega_p$, $\omega_0 = 0.93\omega_p$, and $t_p = 10^{-12}$ s. The amplitude of the gray curve in Fig. 8 is reduced by three times. In the transmitted pulse, shown in Fig. 8, behind the main signal, oscillations are observed, the envelope frequencies of which lie in the terahertz domain $3.3 - 5.3$ THz. These oscillations are due to the nonlinear dependence of the group velocity on frequency for the waves excited by the pulse in plasma.

When a pulse excites waves with the frequencies belonging to the interval (ω_+, ∞), the shape of the transmitted pulse is similar to that which occurs in the case of unmagnetized plasma, when the waves of the range (ω_p, ∞) are excited. In Figs. 9 and 10, we show the same functions as Figs. 3 and 4 but, in the case where $\Omega = 0.25\omega_p$, $\omega_0 = 1.2\omega_p$, and $t_p\omega_p = 18$. The amplitude of the gray curve in Fig. 10 is reduced by a factor of three. In Fig. 10, we demonstrate that the group velocity dependence on frequency leads to a significant broadening of the pulse, and the weak nonlinearity of this dependence near the frequency

ω_+ manifests itself in oscillations behind the pulse.

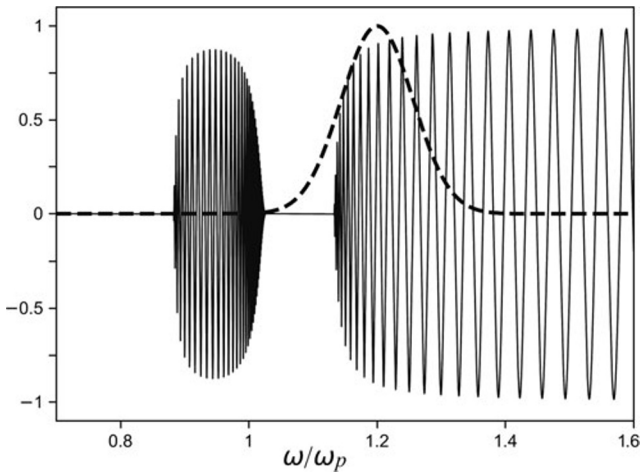

Fig. 9. The real part of transmission coefficient $T(l,\omega)$ (the solid curve) and the Fourier image of the electric component of the incident wave field $E^{\rm inc}(0,\omega)/\sqrt{\pi/2}E_L t_p$ (the dashed curve) on the frequency. The curves are plotted for parameter values $\Omega = 0.25\omega_p$, $\omega_0 = 1.2\omega_p$, and $t_p\omega_p = 18$.

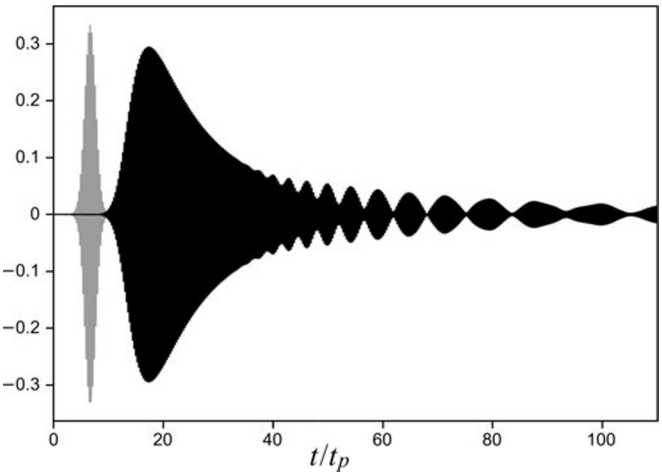

Fig. 10. Time dependences of the transmitted wave field $E(l,t)/E_L$ (the black curve) and the incident wave field $E_{\rm inc}(l,t)/E_L$ passed the distance l in the vacuum (the gray curve). The values of plasma and pulse parameters are $\Omega = 0.25\omega_p$, $\omega_0 = 1.2\omega_p$, and $t_p\omega_p = 18$.

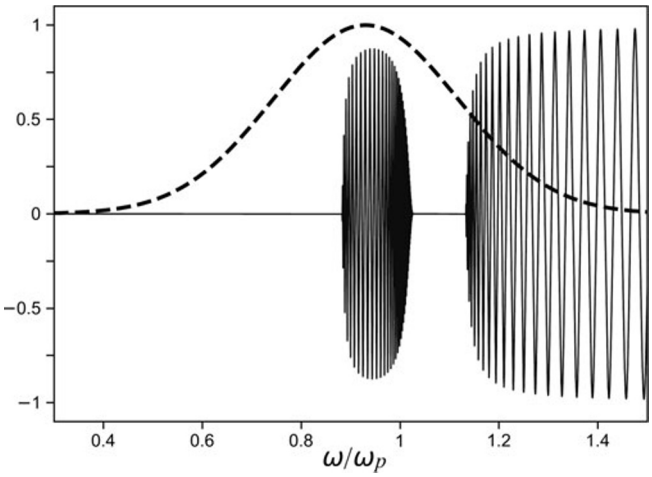

Fig. 11. The real part of transmission coefficient $T(l,\omega)$ (the solid curve) and the Fourier image of the electric component of the incident wave field $E^{\rm inc}(0,\omega)/\sqrt{\pi/2}E_L t_p$ (the dashed curve) on the frequency. The curves are plotted for parameter values $\Omega = 0.25\omega_p$, $\omega_0 = 0.93\omega_p$, $t_p\omega_p = 5.3$.

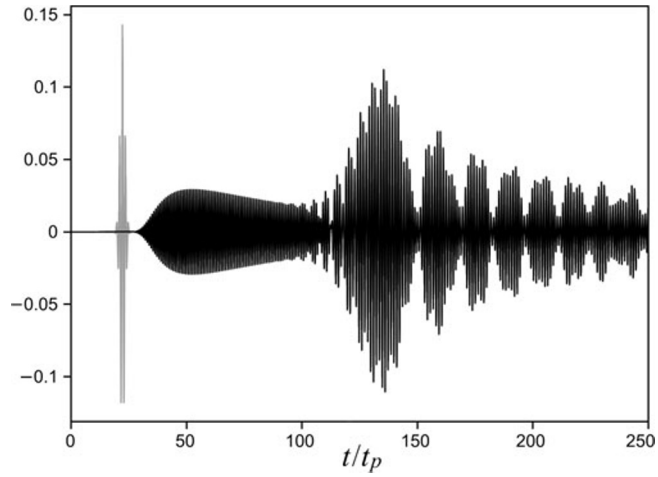

Fig. 12. Time dependences of the transmitted wave field $E(l,t)/E_L$ (the black curve) and the incident wave field $E_{\rm inc}(l,t)/E_L$ passed the distance l in the vacuum (the gray curve). The values of plasma and pulse parameters are $\Omega = 0.25\omega_p$, $\omega_0 = 0.93\omega_p$, and $t_p\omega_p = 5.3$.

In the case of a sufficiently short pulse, a situation is possible where the incident pulse excites waves that simultaneously belong to the transparency regions (ω_-, ω_h) and (ω_+, ∞). In Figs. 11 and 12, we show the same curves as Figs. 3 and 4, respectively, but for $\Omega = 0.25\omega_p$, $\omega_0 = 0.93\omega_p$, and $t_p\omega_p = 5.3$. The amplitude of the gray curve in Fig. 12 is reduced by seven times. In this case, the transmitted pulse

is a superposition of two pulses corresponding to different domains of transparency. One of them is due to higher frequency waves in the region (ω_+, ∞), which have a higher group velocity; as a result, the delay of this pulse compared to a pulse propagating in vacuum over a distance l is several times greater t_p. The second is due to the region (ω_-, ω_h), where the characteristic group velocity is lower and the pulse delay is several tens of times greater t_p. In this case, the pulse broadening, accompanied by a decrease of its amplitude, manifests itself most clearly. In addition, as in the two previous cases, the influence of group velocity nonlinearity near the frequencies ω_-, ω_h, and ω_+ leads to the oscillations appearance in the pulse envelope.

When collisions are taken into account, the amplitude of the transmitted pulse decreases due to energy dissipation inside the plasma layer. Waves with low group velocities have the greatest collisional damping. For this reason, pulses having a carrier frequency near frequencies ω_h or $\omega_\pm$, where the group velocity vanishes, are strongly suppressed. In strong magnetic fields, the influence of the collision frequency is less pronounced. Note that in an optically thin layer, when $l\omega_p \lesssim c$, despite the presence of collisions, there are no noticeable changes in the amplitude of the transmitted pulse.

3. Summary

In this study, we showed to what extent it is possible to control the shape of a Gaussian electromagnetic radiation pulse interacting with a plasma layer located in a constant magnetic field directed along its boundaries. The ability to control the pulse shape was demonstrated in the case of a plasma layer with sharp boundaries. For example, in a weak magnetic field for the plasma parameters under consideration, the time of the layer boundaries blurring is of the order of $\sim c/v_s\omega_p$, where v_s is the speed of sound. This means that, for a pulse duration $t_p \ll c/v_s\omega_p$, the influence of plasma expansion can be neglected. It is enough to implement the conditions for creating a plasma layer in a time less than $c/v_s\omega_p$ and a width of the layer boundary blurring region less than c/ω_p. In a strong magnetic field, it is even easier to implement such conditions, since the magnetic field suppresses the plasma expansion.

References

1. N. G. Borisenko, A. A. Akunets, A. M. Khalenkov, et al., *J. Russ. Laser Res.*, **28**, 548 (2007).
2. R. L. Stenzel and J. M. Urrutia, *J. Appl. Phys.*, **113**, 103303 (2013).
3. H. Zhou, X. Li, K. Xie, et al., *AIP Adv.*, **7**, 025114 (2017).
4. A. Kumar, N. Kumar, and K. B. Thapa, *Eur. Phys. J. Plus*, **133**, 250 (2018).
5. A. V. Bogatskaya, N. V. Klenov, M. V. Tereshonok, et al., *J. Phys. D*, **51**, 185602 (2018).
6. A. V. Bogatskaya, E. A. Volkova, and A. M. Popov, *Laser Phys.*, **29**, 086002 (2019).
7. K. Ohmori, *Ann. Rev. Phys. Chem.*, **60**, 487 (2009).
8. M. Jewariya, M. Nagai, and K. Tanaka, *Phys. Rev. Lett.*, **105**, 203003 (2010).
9. M. Veli, D. Mengu, N. T. Yardimci, et al., *Nat. Commun.*, **12**, 37 (2021).
10. C. F. Hsieh, R. P. Pan, T. T. Tang, et al., *Opt. Lett.*, **31**, 1112 (2006).
11. J. Mork, Y. Chen, and M. Heuck, *Phys. Rev. Lett.*, **113**, 163901 (2014).
12. H. T. Chen, S. Palit, T. Tyler, et al., *Appl. Phys. Lett.*, **93**, 091117 (2008).
13. R. Yan, B. Sensale-Rodriguez, L. Liu, et al., *Opt. Express*, **20**, 28664 (2012).
14. K. N. Ovchinnikov and S. A. Uryupin, *J. Russ. Laser Res.*, **42**, 467 (2019).
15. V. E. Grishkov, K. N. Ovchinnikov, and S. A. Uryupin, *J. Russ. Laser Res.*, **42**, 538 (2021).